

# Localized Dimension Growth: A Convolutional Random Network Coding Approach to Managing Memory and Decoding Delay

Wangmei Guo, Xiaomeng Shi, *Student Member, IEEE*, Ning Cai, *Member, IEEE*, and Muriel Médard, *Fellow, IEEE*

**Abstract**—We consider an *Adaptive Random Convolutional Network Coding* (ARCNC) algorithm to address the issue of field size in random network coding for multicast, and study its memory and decoding delay performances through both analysis and numerical simulations. ARCNC operates as a convolutional code, with the coefficients of local encoding kernels chosen randomly over a small finite field. The cardinality of local encoding kernels increases with time until the global encoding kernel matrices at related sink nodes have full rank. ARCNC adapts to unknown network topologies without prior knowledge, by locally incrementing the dimensionality of the convolutional code. Because convolutional codes of different constraint lengths can coexist in different portions of the network, reductions in decoding delay and memory overheads can be achieved. We show that this method performs no worse than random linear network codes in terms of decodability, and can provide significant gains in terms of average decoding delay or memory in combination, shuttle and random geometric networks.

**Index Terms**—convolutional network codes, random linear network codes, adaptive random convolutional network code, combination networks, random graphs.

## I. INTRODUCTION

SINCE its introduction [1], network coding has been shown to offer advantages in throughput, power consumption, and security in wireline and wireless networks. Field size and adaptation to unknown topologies are two of the key issues in network coding. Li et al. showed constructively that the max-flow bound is achievable by linear algebraic network coding (ANC) if the field is sufficiently large for a given deterministic multicast network [2], while Ho et al. [3] proposed a distributed random linear network code (RLNC) construction that achieves the multicast capacity with probability  $(1 - d/q)^\eta$ , where  $\eta$  is the number of links with random coefficients,  $d$  is the number of sinks, and  $q$  is the field size. Because of its construction simplicity and the ability to

adapt to unknown topologies, RLNC is often preferred over deterministic network codes. While the construction in [3] allows cycles, which leads to the creation of convolutional codes, it does not make use of the convolutional nature of the resulting codes to lighten bounds on field size, which may need to be large to guarantee decoding success at all sinks. Both block network codes (BNC) [4], [5] and convolutional network codes (CNC) [6], [7] can mitigate field size requirements. Médard et al. introduced the concept of BNC [4]; Xiao et al. proposed a deterministic binary BNC to solve the combination network problem [8]. BNC can operate on smaller finite fields, but the block length may need to be pre-determined according to network size. In discussing cyclic networks, both Li et al. and Ho et al. pointed out the equivalence between ANC in cyclic networks with delays, and CNC [2], [3]. Because of coding introduced across the temporal domain, CNC in general does not have a field size constraint.

Combining the adaptive and distributive advantages of RLNC and the field-size independence of CNC, we proposed adaptive random convolutional network code (ARCNC) in [9] as a localized coding scheme for single-source multicast. ARCNC randomly chooses local encoding kernels from a small field, and the code constraint length increases locally at each node. In general, sinks closer to the source adopts a smaller code length than that of sinks far away. ARCNC adapts to unknown network topologies without prior knowledge, and allows convolutional codes with different code lengths to coexist in different portions of the network, leading to reduction in decoding delay and memory overheads associated with using a pre-determined field size or code length.

Concurrently to [9], Ho et al. proposed a variable length CNC [10] and provided a mathematical proof to show that the overall error probability of the code can be bounded when each intermediate node chooses its code length from a range estimated from its depth. The encoding process involves a graph transformation of the network into a “low-degree” form, with each node having a degree of at most 3. Our work differs from [10] in that our approach uses feedbacks algorithmically.

In this paper, we first describe the ARCNC algorithm in acyclic and cyclic networks and show that ARCNC converges in a finite amount of time with probability 1. We then provide several examples to illustrate the decoding delay and memory gains ARCNC offers in deterministic and random networks. Our first example is  $\binom{n}{m}$  combination networks. Ngai and Yeung have previously pointed out that throughput gains of

This work has been partially presented in ISIT 2011.

Wangmei Guo and Ning Cai are with The State Key Laboratory of ISN, Xidian University, Xi’an, China. email: {wangmeiguo, caining}@mail.xidian.edu.cn. This material is based upon work supported by the National Natural Science Foundation of China under Grant No. 60832001.

Xiaomeng Shi and Muriel Médard are with the Research Laboratory of Electronics, Department of Electrical Engineering and Computer Science, Massachusetts Institute of Technology, Cambridge, MA, USA. e-mail: {xshi, medard}@mit.edu. This material is based upon work supported by the Air Force Office of Scientific Research (AFOSR) under award number 016974-002 S, the Claude E. Shannon Research Assitanship from RLE, and by the NSERC Postgraduate Scholarship (PGS) issued by the Natural Sciences and Engineering Research Council of Canada.

network coding can be unbounded over combination networks [11]. Our analysis shows that the average decoding delay is bounded by a constant when  $m$  is fixed and  $n$  increases. In other words, the decoding delay gain becomes infinite as the number of intermediate nodes increases in a combination network. On the other hand, our numerical simulation shows that the decoding delay increases sublinearly when  $m = n/2$  and  $n$  increases in value. We then consider a family of networks defined as *sparsified combination networks* to illustrate the effect of interdependencies among sinks and depth of the network on memory use. For cyclic networks, we consider the shuttle network as an example. We also extend the application of ARCNC from structured cyclic and acyclic networks to random geometric graphs, where we provide empirical illustration of the benefits of ARCNC.

The remainder of this paper is organized as follows: the ARCNC algorithm is proposed in Section II; performance analysis is given in Section III. The coding delay and memory advantages of ARCNC are discussed for combination and shuttle networks in Section IV. Numerical results are provided in Section V for combination and random networks. Section VI concludes the paper.

## II. ADAPTIVE RANDOMIZED CONVOLUTIONAL NETWORK CODES

### A. Basic Model and Definitions

We model a communication network as a finite directed multigraph, denoted by  $\mathcal{G} = (\mathcal{V}, \mathcal{E})$ , where  $\mathcal{V}$  is the set of nodes and  $\mathcal{E}$  is the set of edges. An edge represents a noiseless communication channel with unit capacity. We consider the single-source multicast case, i.e., the source sends the same messages to all the sinks in the network. The source node is denoted by  $s$ , and the set of  $d$  sink nodes is denoted by  $R = \{r_1, \dots, r_d\} \subset \mathcal{V}$ . For every node  $v \in \mathcal{V}$ , the sets of incoming and outgoing channels to  $v$  are  $In(v)$  and  $Out(v)$ ; let  $In(s)$  be the empty set  $\emptyset$ . An ordered pair  $(e', e)$  of edges is called an *adjacent pair* when there exists a node  $v$  with  $e' \in In(v)$  and  $e \in Out(v)$ . Since edges are directed, we use the terms edge and arc interchangeably in this paper.

The symbol alphabet is represented by a base field,  $\mathbb{F}_q$ . Assume  $s$  generates a source *message* per unit time, consisting of a fixed number of  $m$  source *symbols* represented by a size  $m$  row vector  $x_t = (x_{1,t}, x_{2,t}, \dots, x_{m,t})$ ,  $x_{i,t} \in \mathbb{F}_q$ . Time  $t$  is indexed from 0, with the  $(t+1)$ -th message is generated at time  $t$ . The source messages can be collectively represented by a power series  $x(z) = \sum_{t \geq 0} x_t z^t$ , where  $x_t$  is the message generated at time  $t$  and  $z$  denotes a unit-time delay.  $x(z)$  is therefore a row vector of polynomials from the ring  $\mathbb{F}_q[z]$ .

Denote the data propagated over a channel  $e$  by  $y_e(z) = \sum_{t \geq 0} y_{e,t} z^t$ , where  $y_{e,t} \in \mathbb{F}_q$  is the data symbol sent on edge  $e$  at time  $t$ . For edges connected to the source, let  $y_e(t)$  be a linear function of the source messages, i.e., for all  $e \in Out(s)$ ,  $y_e(z) = x(z)f_e(z)$ , where  $f_e(z) = \sum_{t \geq 0} f_{e,t} z^t$  is a size  $m$  column vector of polynomials from  $\mathbb{F}_q[z]$ . For edges not connected directly to the source, let  $y_e(z)$  be a linear function of data transmitted on incoming adjacent edges  $e'$ , i.e., for all

$v \neq s$ ,  $e \in Out(v)$ ,

$$y_e(z) = \sum_{e' \in In(v)} k_{e',e}(z) y_{e'}(z). \quad (1)$$

Both  $k_{e',e}(z)$  and  $y_e(z)$  are in  $\mathbb{F}_q[z]$ . Define  $k_{e',e}(z) = \sum_{t \geq 0} k_{e',e,t} z^t$  as the *local encoding kernel* over the adjacent pair  $(e', e)$ , where  $k_{e',e,t} \in \mathbb{F}_q$ . Thus, for all  $e \in \mathcal{E}$ ,  $y_e(z)$  is a linear function of the source messages,

$$y_e(z) = x(z) f_e(z), \quad (2)$$

where  $f_e(z) = \sum_{t \geq 0} f_{e,t} z^t$  is the size  $m$  column vector defined as the *global encoding kernel* over channel  $e$ , and for all  $v \neq s$ ,  $e \in Out(v)$ ,

$$f_e(z) = \sum_{e' \in In(v)} k_{e',e}(z) f_{e'}(z), \quad (3)$$

$$\text{i.e., } f_{e,t} = \sum_{e' \in In(v)} \left( \sum_{i=0}^t k_{e',e,i} f_{e',t-i} \right). \quad (4)$$

Note that  $f_{e,t} \in \mathbb{F}_q^m$ , and  $f_{e'}(z), f_e(z) \in \mathbb{F}_q^m[z]$ . Expanding Eq. (1) term by term gives an explicit expression for each data symbol  $y_{e,t}$  transmitted on edge  $e$  at time  $t$ , in terms of source symbols and global encoding kernel coefficients:

$$y_{e,t} = \sum_{e' \in In(v)} \left( \sum_{i=0}^t k_{e',e,i} y_{e',t-i} \right) = \sum_{i=0}^t x_{t-i} f_{e,i}. \quad (5)$$

Each intermediate node  $v \neq s$  is therefore required to store in its memory received data symbols  $y_{e',t-i}$  for values of  $i$  at which  $k_{e',e,i}$  is non-zero. The design of a CNC is the process of determining local encoding kernel coefficients  $k_{e',e,t}$  for all adjacent pairs  $(e', e)$ , and  $f_{e,t}$  for  $e \in Out(s)$ , such that the original source messages can be decoded correctly at the given set  $R$  of sink nodes. With a random linear code, these coding kernel coefficients are chosen uniformly randomly from the finite field  $\mathbb{F}_q$ . This paper studies an adaptive scheme where kernel coefficients are generated one at a time until decodability is achieved at all sinks.

Collectively, we call the  $|In(v)| \times |Out(v)|$  matrix  $K_v(z) = (k_{e',e}(z))_{e' \in In(v), e \in Out(v)} = K_{v,0} + K_{v,1}z + K_{v,2}z^2 + \dots$  the *local encoding kernel matrix* at node  $v$ , and the  $m \times |In(v)|$  matrix  $F_v(z) = (f_e(z))_{e \in In(v)}$  the *global encoding kernel matrix* at node  $v$ . Observe from Eq. (2) that, at sink  $r$ ,  $F_r(z)$  is required to deconvolve the received data messages  $y_{e'_i}(z)$ ,  $e'_i \in In(r)$ . Therefore, each intermediate node  $v$  computes  $f_e(z)$  for outgoing edges from  $F_v(z)$  according to Eq.(3), and sends  $f_e(z)$  along edge  $e$ , together with data  $y_e(z)$ . This can be achieved by arranging the coefficients of  $f_e(z)$  in a vector form and attaching them to the data. In this paper, we ignore the effect of this overhead transmission of coding coefficients on throughput or delay: we show in Section III-B that the number of terms in  $f_e(z)$  is finite, thus the overhead can be amortized over a long period of data transmissions.

Moreover,  $F_v(z)$  can be written as  $F_v(z) = F_{v,0} + F_{v,1}z + \dots + F_{v,t}z^t$ , where  $F_{v,t} \in \mathbb{F}_q^{m \times |In(v)|}$  is the global encoding kernel matrix at time  $t$ .  $F_v(z)$  can thus be viewed as a polynomial, with  $F_{v,t}$  as matrix coefficients. Let  $L_v$  be the degree of  $F_v(z)$ .  $L_v + 1$  is a direct measure of the amount of memory

required to store  $F_v(z)$ . We shall define in Section III-C the metric used to measure memory overhead of ARCNC.

### B. Algorithm for Acyclic Networks

1) *Code Generation and Data Encoding*: initially, all local and global encoding kernels are set to 0. At time  $t$ , the  $(t+1)$ -th coefficient  $k_{e',e,t}$  of the local encoding kernel  $k_{e',e}(z)$  is chosen uniformly randomly from  $\mathbb{F}_q$  for each adjacent pair  $(e', e)$ , independently from other kernel coefficients. Each node  $v$  stores the local encoding kernels and forms the outgoing data symbol as a random linear combination of incoming data symbols in its memory according to Eq. (5). Node  $v$  also stores the global encoding kernel matrix  $F_v(z)$  and computes the global encoding kernel  $f_e(z)$ , in the form of a vector of coding coefficients, according to Eq. (3). During this code construction process,  $f_e(z)$  is attached to the data transmitted on  $e$ . Once code generation terminates and the CNC  $F_r(z)$  is known at each sink  $r$ ,  $f_e(z)$  no longer needs to be forwarded, and only data symbols are sent on each outgoing edge. Recall that we ignore the reduction in rate due to the transmission of coding coefficients, since this overhead can be amortized over long periods of data transmissions.

In acyclic networks, a complete topological order exists among the nodes, starting from the source. Edges can be ranked such that coding can be performed sequentially, where a downstream node encodes after all its upstream nodes have generated their coding coefficients. Observe that we have not assumed non-zero transmission delays.

2) *Testing for Decodability and Data Decoding*: at every time instant  $t$ , each sink  $r$  decides whether its global encoding kernel matrix  $F_r(z)$  is full rank. If so, it sends an ACK signal to its parent node. An intermediate node  $v$  which has received ACKs from all its children at time  $t_0$  will send an ACK to its parent, and set all subsequent local encoding kernel coefficients  $k_{e',e,t}$  to 0 for all  $t > t_0$ ,  $e' \in In(v)$ , and  $e \in Out(v)$ . In other words, the constraint lengths of the local convolutional codes increase until they are sufficient for downstream sinks to decode successfully. Such automatic adaptation eliminates the need for estimating the field size or the constraint length a priori. It also allows nodes within the network to operate with different constraint lengths as needed.

If  $F_r(z)$  is not full rank,  $r$  stores received messages and waits for more data to arrive. At time  $t$ , the algorithm is considered successful if all sinks can decode. This is equivalent to saying that the determinant of  $F_r(z)$  is a non-zero polynomial. Recall from Section II-A,  $F_r(z)$  can be written as  $F_r(z) = F_{r,0} + F_{r,1}z + \dots + F_{r,t}z^t$ , where  $F_{r,t}$  is the global encoding kernel matrix at time  $t$ . Computing the determinant of  $F_r(z)$  at every time instant  $t$  is complex, so we test instead the following two conditions, introduced in [12] and [13] to determine decodability at a sink  $r$ . The first condition is necessary and easy to compute, while the second is both necessary and sufficient, but slightly more complex.

1)  $rank(\widehat{F}_{r,t}) = m$ , where  $\widehat{F}_{r,t} = (F_{r,0}, F_{r,1}, \dots, F_{r,t})$ .

2)  $rank(M_{r,t}) - rank(M_{r,t-1}) = m$ , where

$$M_{r,i} = \begin{pmatrix} F_{r,0} & F_{r,1} & \dots & F_{r,i} \\ 0 & \ddots & \ddots & \vdots \\ 0 & \dots & F_{r,0} & F_{r,1} \\ 0 & \dots & 0 & F_{r,0} \end{pmatrix}. \quad (6)$$

Once  $F_r(z)$  is full rank,  $r$  can perform decoding operations. Let  $T_r$  be the *first decoding time*, or the earliest time at which the decodability conditions are satisfied. Denote by  $x_0^{T_r}$  and  $y_0^{T_r}$  the row vectors  $(x_0, \dots, x_{T_r})$  and  $(y_0, \dots, y_{T_r})$ . Each source message  $x_t$  is a size  $m$  row vector of source symbols  $x_{i,t} \in \mathbb{F}_q$  generated at  $s$  at time  $t$ ; each data message  $y_t$  is a size  $In(r)$  row vector of data symbols  $y_{e,t} \in \mathbb{F}_q$  received on the incoming edges of  $r$  at time  $t$ ,  $e \in In(r)$ . Hence,  $y_0^{T_r} = x_0^{T_r} M_{T_r}$ . To decode, we want to find a size  $In(r)(T_r+1) \times m$  matrix  $D$  such that  $M_{T_r} D = \begin{pmatrix} I_m \\ 0 \end{pmatrix}$ . We can then recover source message  $x_0$  by evaluating  $y_0^{T_r} D = x_0^{T_r} M_{T_r} D = x_0$ . Once  $D$  is determined, we can decode sequentially the source message  $x_t$  at time  $t + T_r$ ,  $t > 0$ . Note that if  $|In(r)| > m$ , we can simplify the decoding process by using only  $m$  independent received symbols from the  $|In(r)|$  incoming edges.

Observe that, an intermediate node  $v$  only stops lengthening its local encoding kernels  $k_{e',e}(z)$  when *all* of its downstream sinks achieve decodability. Thus, for a sink  $r$  with first decoding time  $T_r$ , the length of  $F_r(z)$  can increase even after  $T_r$ . Recall from Section II-A that  $L_r$  is the degree of  $F_r(z)$ . We will show in Section III-B that ARCNC converges in a finite amount of time for a multicast connection. In other words, when the decodability conditions are satisfied at *all* sinks, the values of  $L_r$  and  $T_r$  at an individual sink  $r$  satisfy the condition  $L_r \geq T_r$ , where  $L_r$  is finite. Decoding of symbols after time  $T_r$  can be conducted sequentially. Details of the decoding operations can be found in [14].

3) *Feedback*: As we have described in the decoding subsection, acknowledgments are propagated from sinks through intermediate nodes to the source to indicate if code length should continue to be increased at coding nodes. ACKs are assumed to be instantaneous and require no dedicated network links, thus incurring no additional delay or throughput costs. Such assumptions may be reasonable in many systems since feedback is only required during the code construction process. Once code length adaptation finishes, ACKs are no longer needed. We show in Section III-B that ARCNC terminates in a finite amount of time. Therefore, the cost of feedback can be amortized over periods of data transmissions.

### C. Algorithm Statement for Cyclic Networks

In an acyclic network, the local and global encoding kernel descriptions of a linear network code are equivalent, in the sense that for a given set of local encoding kernels, a set of global encoding kernels can be calculated recursively in any upstream-to-downstream order. In other words, a code generated from local encoding kernels has a unique solution when decoding is performed on the corresponding global encoding kernels. By comparison, in a cyclic network, partial orderings of edges or nodes are not always consistent. Given a set of local encoding kernels, there may exist a unique, none,

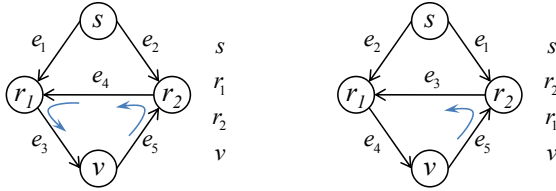


Fig. 1. A sample cyclic network with edges numerically indexed. The set of indices is not unique, and depends on the order at which nodes are visited, starting from  $s$ . On the left,  $r_1$  is visited before  $r_2$ ; on the right,  $r_2$  is visited before  $r_1$ . In each case,  $(e', e)$  is highlighted with a curved arrow if  $e' \succeq e$ .

or multiple sets of global encoding kernels (§3.1, [15]). If the code is non-unique, the decoding process at a sink may fail. A sufficient condition for a CNC to be successful is that the constant coefficient matrix consisting of all local encoding kernels be nilpotent [16]; this condition is satisfied if we code over an acyclic topology at  $t = 0$  [12]. In the extreme case, all local encoding kernels can be set to 0 at  $t = 0$ . This setup translates to a unit transmission delay on each link, which as previous work on RLNC has shown, guarantees the uniqueness of a code construction [3]. To minimize decoding delay, it is intuitive to make as few local encoding kernels zero as possible. In other words, a reasonable heuristic is to assign 0 to a minimum number of  $k_{e',e,0}$ ,  $(e', e) \in \mathcal{E}$ , and to assign values chosen uniformly randomly from  $\mathbb{F}_q$  to the rest. The goal is to guarantee that each cycle contains at least a single delay.

Although seemingly similar, this process is actually not the same as the problem of finding the minimal feedback edge set. A feedback edge set is a set containing at least one edge of every cycle in the graph. When a feedback edge set is removed, the graph becomes an acyclic directed graph. In our setup, however, since  $k_{e',e,0}$  is specific to an adjacent edge pair,  $k_{e',e,0}$  does not need to be 0 for all  $e'$  where  $(e', e) \in \mathcal{V}$ .

For example, a very simple but not necessarily delay-optimal heuristic is to index all edges, and to assign 0 to  $k_{e',e,0}$  if  $e' \succeq e$ , i.e., when  $e'$  has an index larger than  $e$ ;  $k_{e',e,0}$  is chosen randomly from  $\mathbb{F}_q$  if  $e' \prec e$ . Fig. 1 illustrates this indexing scheme. A node is considered to be visited if one of its incoming edges has been indexed; a node is put into a queue once it is visited. For each node removed from the queue, numerical indices are assigned to all of its outgoing edges. Nodes are traversed starting from the source  $s$ . The outgoing edges of  $s$  are therefore numbered from 1 to  $|Out(s)|$ . Note that the index set thus obtained is not necessarily unique. In this particular example, we can have two sets of edge indices, as shown in Fig. 1. Here  $r_1$  is visited before  $r_2$  on the left, and vice versa on the right. In each case, an adjacent pair  $(e', e)$  is highlighted with a curved arrow if  $e' \succeq e$ . At  $t = 0$ , we set  $k_{e',e,0}$  to 0 for such highlighted adjacent pairs, and choose  $k_{e',e,0}$  uniformly randomly from  $\mathbb{F}_q$  for other adjacent pairs.

Observe that, in an acyclic network, this indexing scheme provides a total ordering for the nodes as well as for the edges: a node is visited only after all of its parents and ancestors are visited; an edge is indexed only after all edges on any of its paths from the source are indexed. In a cyclic network, however, an order of nodes and edges is only partial,

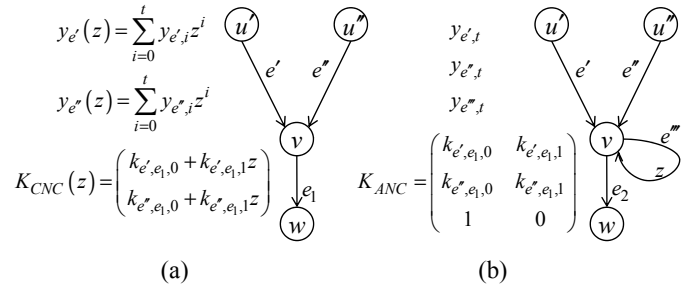


Fig. 2. A convolution code resulting from self-loops on a network with transmission delays. (a) CNC in a delay-free network. Data transmitted on incoming edges are  $y_{e'}(z)$  and  $y_{e''}(z)$  respectively. The local encoding kernels are given by  $K_{CNC}(z)$ . (b) Equivalent ANC in a network with delays. The given self-loop carries a single delay  $z$ . Incoming data symbols are  $y_{e',t}$  and  $y_{e'',t}$  at time  $t$ . The ANC coding coefficients are given by the matrix  $K_{ANC}$ .

with inconsistencies around each cycle. Such contradictions in the partial ordering of edges make the generation of unique network codes along each cycle impossible. By assigning 0 to local encoding kernels  $k_{e',e,0}$  for which  $e' \succeq e$ , such inconsistencies can be avoided at time 0, since the order of  $e'$  and  $e$  becomes irrelevant in determining the network code. After the initial step,  $k_{e',e,t}$  is not necessarily 0 for  $e' \succeq e$ ,  $t > 0$ , nonetheless the convolution operations at intermediate nodes ensure that the 0 coefficient inserted at  $t = 0$  makes the global encoding kernels unique at the sinks. This idea can be derived from the expression for  $f_{e,t}$  given in Eq. (4). In each cycle, there is at least one  $k_{e',e,0}$  that is equal to zero. The corresponding  $f_{e',t}$  therefore does not contribute to the construction of other  $f_{e,t}$ 's in the cycle. In other words, the partial ordering of arcs in the cycle can be considered consistent at  $t = 1$  and later times.

Although this heuristic for cyclic networks is not optimal, it is universal. One disadvantage of this approach is that full knowledge of the topology is required at  $t = 0$ , making the algorithm centralized instead of entirely distributed. Nonetheless, if inserting an additional transmission delay on each link is not an issue, we can always bypass this code assignment stage by zeroing all local encoding kernels at  $t = 0$ .

After initialization, the algorithm proceeds in exactly the same way as in the acyclic case.

### III. ANALYSIS

#### A. Success probability

Discussions in [2], [3], [16] state that in a network with delays, ANC gives rise to random processes which can be written algebraically in terms of a delay variable  $z$ . Thus, a convolutional code can naturally evolve from message propagation and linear encoding. ANC in the delay-free case is therefore equivalent to CNC with constraint length 1. Similarly, using a CNC with constraint length  $l > 1$  on a delay-free network is equivalent to performing ANC on the same network, but with  $l - 1$  self-loops attached to each encoding node. Each self-loop carries  $z, z^2, \dots, z^{l-1}$  units of delay respectively.

For example, in Fig. 2, we show a node with two incoming edges. Let the data symbol transmitted on edge  $e$  at time  $t$  be  $y_{e,t}$ . A CNC with length  $l = 2$  is used in (a), assuming that

transmissions are delay-free. The local encoding kernel matrix  $K_{\text{CNC}}(z)$  contains two polynomials,  $k_{e',e_1}(z) = k_{e',e_1,0} + k_{e',e_1,1}z$  and  $k_{e'',e_1}(z) = k_{e'',e_1,0} + k_{e'',e_1,1}z$ . According to Eq. (1) and (5), the data symbol transmitted on  $e_1$  at time  $t$  is

$$y_{e_1,t} = \sum_{\dot{e} \in \{e',e''\}} y_{\dot{e},t} k_{\dot{e},e_1,0} + y_{\dot{e},t-1} k_{\dot{e},e_1,1}. \quad (7)$$

In (b), the equivalent ANC is shown. A single loop with a transmission delay of  $z$  has been added, and the local encoding kernel matrix  $K_{\text{ANC}} = (k_{\dot{e},e})_{\dot{e} \in \text{In}(v), e \in \text{Out}(v)}$  is constructed from coding coefficients from (a). The first column of  $K_{\text{ANC}}$  represents encoding coefficients from incoming edges  $e', e'', e'''$  to the outgoing edge  $e_2$ , and the second column represents encoding coefficients from incoming edges  $e', e'', e'''$  to the outgoing edge  $e'''$ . Using a matrix notation, the output data symbols from  $v$  are  $(y_{e_2,t} \ y_{e''',t}) = (y_{e',t} \ y_{e'',t} \ y_{e''',t-1}) K_{\text{ANC}}$ , i.e.,

$$\begin{aligned} y_{e''',t} &= y_{e',t} k_{e',e'''} + y_{e'',t} k_{e'',e'''} + y_{e''',t-1} k_{e''',e'''} \\ &= y_{e',t} k_{e',e_1,1} + y_{e'',t} k_{e'',e_1,1} \\ y_{e_2,t} &= y_{e',t} k_{e',e_2} + y_{e'',t} k_{e'',e_2} + y_{e''',t-1} k_{e''',e_2} \\ &= y_{e',t} k_{e',e_1,0} + y_{e'',t} k_{e'',e_1,0} + y_{e''',t-1} \\ &= \sum_{\dot{e} \in \{e',e''\}} y_{\dot{e},t} k_{\dot{e},e_1,0} + y_{\dot{e},t-1} k_{\dot{e},e_1,1} \end{aligned} \quad (8)$$

Clearly  $y_{e_1,t}$  is equal to  $y_{e_2,t}$ . ARCNC therefore falls into the framework given by Ho et al. [3], in the sense that the convolution process either arises naturally from cycles with delays, or can be considered as computed over self-loops appended to acyclic networks. Applying the analysis from [3], we have the following theorem,

*Theorem 1:* For multicast over a general network with  $d$  sinks, the ARCNC algorithm over  $\mathbb{F}_q$  can achieve a success probability of at least  $(1 - d/q^{t+1})^\eta$  at time  $t$ , if  $q^{t+1} > d$ , and  $\eta$  is the number of links with random coefficients.

*Proof:* At node  $v$ ,  $k_{e',e}(z)$  at time  $t$  is a polynomial with maximal degree  $t$ , i.e.,  $k_{e',e}(z) = k_{e',e,0} + k_{e',e,1}z + \dots + k_{e',e,t}z^t$ ,  $k_{e',e,i}$  is randomly chosen over  $\mathbb{F}_q$ . If we group the coefficients, the vector  $k_{e',e} = \{k_{e',e,0}, k_{e',e,1}, \dots, k_{e',e,t}\}$  is of length  $t+1$ , and corresponds to a random element over the extension field  $\mathbb{F}_{q^{t+1}}$ . Using the result in [3], we conclude that the success probability of ARCNC at time  $t$  is at least  $(1 - d/q^{t+1})^\eta$ , as long as  $q^{t+1} > d$ . ■

We could similarly consider the analysis done by Balli et al. [17], which states that the success probability is at least  $(1 - d/(q-1))^{|J|+1}$ ,  $|J|$  being the number of encoding nodes, to show that a tighter lower bound can be given on the success probability of ARCNC, when  $q^{t+1} > d$ .

## B. First decoding time

As discussed in Section II-B2, we define the *first decoding time*  $T_r$  for sink  $r$ ,  $1 \leq r \leq d$ , as the time it takes  $r$  to achieve decodability for the first time. We had called this variable the *stopping time* in [9]. Also recall that when all sinks are able to decode, at each sink  $r$ ,  $T_r$  can be smaller than  $L_r$ , the degree of the global encoding kernel matrix  $F_r(z)$ . Denote by  $T_N$  the time it takes for all sinks in the network to successfully

decode, i.e.,  $T_N = \max\{T_1, \dots, T_d\}$ , then  $T_N$  is also equal to  $\max\{L_1, \dots, L_d\}$ . The following corollary holds:

*Corollary 2:* For any given  $0 < \varepsilon < 1$ , there exists a  $T_0 > 0$  such that for any  $t \geq T_0$ , ARCNC solves the multicast problem with probability at least  $1 - \varepsilon$ , i.e.,  $P(T_N > t) < \varepsilon$ .

*Proof:* Let  $T_0 = \lceil \log_q d - \log_q(1 - \sqrt[t]{1 - \varepsilon}) \rceil - 1$ , then  $T_0 + 1 \geq \lceil \log_q d \rceil$  since  $0 < \varepsilon < 1$ , and  $(1 - d/q^{T_0+1})^\eta > 1 - \varepsilon$ . Applying Theorem 1 gives  $P(T_N > t) \leq P(T_N > T_0) < 1 - (1 - d/q^{t+1})^\eta < \varepsilon$  for any  $t \geq T_0$ . ■

Since  $\Pr\{\cup_{i=t}^\infty [T_N \leq i]\} = 1 - \Pr\{\cap_{i=t}^\infty [T_N > i]\} > 1 - \varepsilon$ , Corollary 2 shows that ARCNC converges and stops in a finite amount of time with probability 1 for a multicast connection.

Another relevant measure of the performance of ARCNC is the *average first decoding time*,  $T_{\text{avg}} = \frac{1}{d} \sum_{r=1}^d T_r$ . Observe that  $E[T_{\text{avg}}] \leq E[T_N]$ , where

$$\begin{aligned} E[T_N] &= \sum_{t=1}^{\lceil \log_q d \rceil - 1} P(T_N \geq t) + \sum_{t=\lceil \log_q d \rceil}^{\infty} P(T_N \geq t) \\ &\leq \lceil \log_q d \rceil - 1 + \sum_{t=\lceil \log_q d \rceil}^{\infty} [1 - (1 - \frac{d}{q^t})^\eta] \\ &= \lceil \log_q d \rceil - 1 + \sum_{k=1}^{\eta} (-1)^{k-1} \binom{\eta}{k} \frac{d^k}{q^{\lceil \log_q d \rceil k - 1}}. \end{aligned}$$

When  $q$  is large, the summation term approximates  $1 - (1 - d/q)^\eta$  by the binomial expansion. Hence as  $q$  increases, the second term above decreases to 0, while the first term  $\lceil \log_q d \rceil - 1$  is 0.  $E[T_{\text{avg}}]$  is therefore upper-bounded by a term converging to 0; it is also lower bounded by 0 because at least one round of random coding is required. Therefore,  $E[T_{\text{avg}}]$  converges to 0 as  $q$  increases. In other words, if the field size is large enough, ARCNC reduces in effect to RLNC.

Intuitively, the average first decoding time of ARCNC depends on the network topology. In RLNC, all nodes are required in code in finite fields of the same size; thus the effective field size is determined by the worst case sink. This scenario corresponds to having all nodes stop at  $T_N$  in ARCNC. ARCNC enables each node to decide locally what is a good constraint length to use, depending on side information from downstream nodes. Since  $E[T_{\text{avg}}] \leq E[T_N]$ , some nodes may be able to decode before  $T_N$ . The corresponding effective field size is therefore expected to be smaller than in RLNC. Two possible consequences of a smaller effective field size are reduced decoding delay, and reduced memory requirements. In Section IV, we confirm through simulations that such gains can be attained by ARCNC.

## C. Memory

To measure the amount of memory required by ARCNC, first recall from Section II-A that at each node  $v$ , the global encoding kernel matrix  $F_v(z)$ , the local encoding kernel matrix  $K_v(z)$ , and past data  $y_{e'}(z)$  on incoming arcs  $e' \in \text{In}(v)$  need to be stored in memory.  $K_v(z)$  and  $y_{e'}(z)$  should always be saved because together they generate new data symbols to transmit (see Eqs. (1) and (5)).  $F_v(z)$  should be saved during the code construction process at intermediate nodes, and always at sinks, since they are needed for decoding.

Let us consider individually the three contributors to memory use. Firstly, recall from Section II-A that  $F_v(z)$  can be viewed as a polynomial in  $z$ . When all sinks are able to decode, at node  $v$ ,  $F_v(z)$  has degree  $L_v$ , with coefficients from  $\mathbb{F}_q^{m \times In(v)}$ . The total amount of memory needed for  $F_v(z)$  is therefore proportional to  $\lceil \log_2 q \rceil m In(v) (L_v + 1)$ . Secondly, from Eq. (4), we see that the length of a local encoding kernel polynomial  $k_{e',e}(z)$  should be equal to or smaller than that of  $f_e(z)$ . Thus, the length of  $K_v(z)$  should also be equal to or smaller than that of  $F_v(z)$ . The coefficients of  $K_v(z)$  are elements of  $\mathbb{F}_q^{In(v) \times Out(v)}$ . Hence, the amount of memory needed for  $K_v(z)$  is proportional to  $\lceil \log_2 q \rceil Out(v) In(v) (L_v + 1)$ . Lastly, a direct comparison between Eqs. (4) and (5) shows that memory needed for  $y_{e'}(z)$ ,  $e' \in In(v)$  is the same for that needed for  $F_v(z)$ . In practical uses of network coding, data can be transmitted in packets, where symbols are concatenated and operated upon in parallel. Packets can be very long in length. Nonetheless, the exact packet size is irrelevant for comparing memory use between different network codes, since all comparisons are naturally normalized to packet lengths.

Observe that,  $m$  is the number of symbols in the source message, determined by the min-cut of the multicast connection, independent of the network code used. Similarly,  $In(v)$  and  $Out(v)$  are attributes inherent to the network topology. To compare the memory use of different network codes, we can omit these terms, and define the average memory use of ARCNC by the following common factor:

$$W_{\text{avg}} \triangleq \frac{\lceil \log_2 q \rceil}{|\mathcal{V}|} \sum_{v \in \mathcal{V}} (L_v + 1). \quad (9)$$

In RLNC,  $L_v = 0$ , and the expression simplifies to  $\lceil \log_2 q \rceil$ , which is the amount of memory needed for a single finite field element.

One point to keep in mind when measuring memory use is that even after a sink achieves decodability, its code length can still increase, as long as at least one of its ancestors has not stopped increasing code length. We say a non-source node  $v$  is *related* to a sink  $r$  if  $v$  is an ancestor of  $r$ , or if  $v$  shares an ancestor, other than the source, with  $r$ . Hence,  $L_r$  is dependent on all nodes related to  $r$ .

#### D. Complexity

To study the computation complexity of ARCNC, first observe that, once the adaptation process terminates, the computation needed for the ensuing code is no more than a regular CNC. In fact, the expected computation complexity is proportional to the average code length of ARCNC. We therefore omit the details of the complexity analysis of regular CNC here and refer interested readers to [7].

For the adaptation process, the encoding operations are described by Eq. (4). If the algorithm stops at time  $T_N$ , the number of operations in the encoding steps is  $O(D_{in} |\mathcal{E}| T_N^2 m)$ , where  $D_{in} = \max_{v \in \mathcal{V}} |In(v)|$ .

To determine decodability at a sink  $r$ , we check if the rank of  $F_r(z)$  is  $m$ . A straight-forward approach is to check whether its determinant is a non-zero polynomial. Alternatively, Gaussian elimination could be applied. At time  $t$ , because  $F_r(z)$

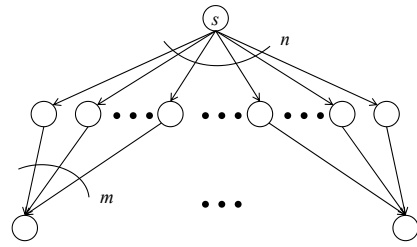


Fig. 3. A combination network

is an  $m \times |In(r)|$  matrix and each entry is a polynomial with degree  $t$ , the complexity of checking whether  $F_r(z)$  is full rank is  $O(D_{in}^2 2^m m t^2)$ . Instead of computing the determinant or using Gaussian elimination directly, we propose to check the conditions given in Section II-B. For each sink  $r$ , at time  $t$ , determining  $rank(F_0 \ F_1 \ \dots \ F_t)$  requires  $O(D_{in}^2 m t^2)$  operations. If the first test passes, we calculate  $rank(M_t)$  and  $rank(M_{t-1})$  next. Observe that  $rank(M_{t-1})$  was computed during the last iteration.  $M_t$  is a  $(t+1)m \times (t+1)|In(r)|$  matrix over field  $\mathbb{F}_q$ . The complexity of calculating  $rank(M_t)$  by Gaussian elimination is  $O(D_{in}^2 m t^3)$ . The process of checking decodability is performed during the adaptation process only, hence the computation complexity here can be amortized over time after the coding coefficients are determined. In addition, as decoding occurs symbol-by-symbol, the adaptation process itself does not impose any additional delays.

## IV. EXAMPLES

In this section, we describe the application of ARCNC in three structured networks: the combination and sparsified combination networks, which are acyclic, and the shuttle network, which is cyclic. For the combination network, we bound the expected average first decoding time; for the sparsified combination network, we bound the expected average memory requirement. In addition, the shuttle network is given as a very simple example to illustrate how ARCNC can be applied in cyclic networks.

### A. Combination Network

A  $\binom{n}{m}$  combination network contains a single source  $s$  that multicasts  $m$  independent messages over  $\mathbb{F}_q$  through  $n$  intermediate nodes to  $d$  sinks [15]; each sink is connected to a distinct set of  $m$  intermediate nodes, and  $d = \binom{n}{m}$ . Fig. 3 illustrates the topology of a combination network. Assuming unit capacity links, the min-cut to each sink is  $m$ . It can be shown that, in combination networks, routing is insufficient and network coding is needed to achieve the multicast capacity  $m$ . Here coding is performed only at  $s$ , since each intermediate node has only  $s$  as a parent node; an intermediate node simply relays to its children data from  $s$ . For a general  $\binom{n}{m}$  combination network, we showed in [9] that the expected average first decoding time can be significantly improved by ARCNC when compared to the deterministic BNC algorithm. We restate the results here, with details of the derivations included.

At time  $t - 1$ , for a sink  $r$  that has not satisfied the decodability conditions,  $F_r(z)$  is a size  $m \times m$  matrix of polynomials of degree  $t - 1$ .  $F_r(z)$  has full rank with probability

$$\begin{aligned} Q &= (q^{tm} - 1)(q^{tm} - q^t) \cdots (q^{tm} - q^{t(m-1)})/q^{tm^2} \\ &= \left(1 - \frac{1}{q^{tm}}\right) \left(1 - \frac{1}{q^{t(m-1)}}\right) \cdots \left(1 - \frac{1}{q^t}\right) \\ &= \prod_{l=1}^m \left(1 - \frac{1}{q^{tl}}\right). \end{aligned} \quad (10)$$

Hence, the probability that sink  $r$  decodes after time  $t - 1$  is

$$P(T_r \geq t) = 1 - Q = 1 - \prod_{l=1}^m \left(1 - \frac{1}{q^{tl}}\right), \quad t \geq 0. \quad (11)$$

The expected first decoding time for sink node  $r$  is therefore upper and lower-bounded as follows.

$$\begin{aligned} E[T_r] &= \sum_{t=1}^{\infty} tP(T_r = t) = \sum_{t=1}^{\infty} P(T_r \geq t) \\ &= \sum_{t=1}^{\infty} \left(1 - \prod_{i=1}^m \left(1 - \frac{1}{q^{tr}}\right)\right) \end{aligned} \quad (12)$$

$$< \sum_{t=1}^{\infty} \left(1 - \left(1 - \frac{1}{q^t}\right)^m\right) \quad (13)$$

$$= \sum_{t=1}^{\infty} \left(1 - \sum_{k=0}^m (-1)^k \binom{m}{k} \left(\frac{1}{q^t}\right)^k\right) \quad (14)$$

$$= \sum_{k=1}^m (-1)^{k-1} \binom{m}{k} \left(\sum_{t=1}^{\infty} \frac{1}{q^{tk}}\right) \quad (15)$$

$$= \sum_{k=1}^m (-1)^{k-1} \binom{m}{k} \frac{1}{q^k - 1} \triangleq ET_{UB}(m, q). \quad (16)$$

$$E[T_r] = \sum_{t=1}^{\infty} \left(1 - \prod_{l=1}^m \left(1 - \frac{1}{q^{tl}}\right)\right) \quad (17)$$

$$> \sum_{t=1}^{\infty} \left(1 - \left(1 - \frac{1}{q^{tm}}\right)^m\right) \quad (18)$$

$$= \sum_{k=1}^m (-1)^{k-1} \binom{m}{k} \frac{1}{q^{km} - 1} \triangleq ET_{LB}(m, q). \quad (19)$$

Recall from Section III-B that the expected average first decoding time is  $E[T_{\text{avg}}] = E\left[\frac{1}{d} \sum_{r=1}^d T_r\right]$ . In a combination network,  $E[T_{\text{avg}}]$  is equal to  $E[T_r]$ . Consequently,  $E[T_{\text{avg}}]$  is upper-bounded by  $ET_{UB}$ , defined by Eq. (16).  $ET_{UB}$  is a function of  $m$  and  $q$  only, independent of  $n$ . For example, if  $m = 2$ ,  $q = 2$ ,  $ET_{UB} = \frac{5}{3}$ . If  $m$  is fixed, but  $n$  increases,  $E[T_{\text{avg}}]$  does not change. In addition, if  $q$  is large,  $ET_{UB}$  becomes 0, consistent with the general analysis in [9].

Next, we want to bound the variance of  $T_{\text{avg}}$ , i.e.,

$$\begin{aligned} \text{var}[T_{\text{avg}}] &= E[T_{\text{avg}}^2] - E^2[T_{\text{avg}}] \\ &= E\left[\left(\frac{1}{d} \sum_{r=1}^d T_r\right)^2\right] - E^2[T_r] \\ &= \frac{E[T_r^2]}{d} + \left(\sum_{r=1}^d \sum_{r' \neq r} \frac{E(T_r T_{r'})}{d^2}\right) - E^2[T_r]. \end{aligned} \quad (20)$$

We upper-bound the terms above one by one. First,

$$E[T_r^2] = \sum_{t=1}^{\infty} t^2 P(T_r = t) \quad (21)$$

$$= \sum_{t=1}^{\infty} t^2 (P(T_r \geq t) - P(T_r \geq t+1)) \quad (22)$$

$$= \sum_{t=1}^{\infty} ((t+1)^2 - t^2) P(T_r \geq t) \quad (23)$$

$$< \sum_{t=1}^{\infty} (2t+1) \left(1 - \left(1 - \frac{1}{q^t}\right)^m\right) \quad (24)$$

$$< ET_{UB} + 2 \sum_{k=1}^m (-1)^{k-1} \binom{m}{k} \sum_{t=1}^{\infty} \frac{t}{q^{tk}} \quad (25)$$

$$= ET_{UB} + 2 \sum_{k=1}^m (-1)^{k-1} \binom{m}{k} \left(\frac{q^k}{q^k - 1}\right)^2 \quad (26)$$

$$\triangleq (ET^2)_{UB} \quad (27)$$

Eq. (23) follows through organization and simplifying. Eq. (24) is obtained by replacing the terms in Eq. (23) with the upperbound of Eq. (10). We represent Eq. (24) with binomial expansion and substitute with the upperbound in Eq. (16). Next, let  $\rho_\lambda = E[T_r T_{r'}]$  if sinks  $r$  and  $r'$  share  $\lambda$  parents,  $0 \leq \lambda < m$ . Thus,  $\rho_0 = E^2[T_r]$ . When  $\lambda \neq 0$ , given sink  $r$  succeeds in decoding at time  $t_1$ , the probability that sink  $r'$  has full rank before  $t_2$  is lower-bounded as follows,

$$P(T_{r'} < t_2 | T_r = t_1) > \prod_{l=1}^{m-\lambda} \left(1 - \frac{1}{q^{t_2 l}}\right) > \left(1 - \frac{1}{q^{t_2}}\right)^{m-\lambda}. \quad (28)$$

Consequently, if  $\lambda \neq 0$ ,

$$\rho_\lambda = E[T_r T_{r'}] \quad (29)$$

$$= \sum_{t_1=1}^{\infty} \sum_{t_2=t_1}^{\infty} t_1 t_2 P(T_r = t_1) P(T_{r'} = t_2 | T_r = t_1) \quad (30)$$

$$= \sum_{t_1=1}^{\infty} t_1 P(T_r = t_1) \sum_{t_2=1}^{\infty} P(T_{r'} \geq t_2 | T_r = t_1) \quad (31)$$

$$< \sum_{t_1=1}^{\infty} t_1 P(T_r = t_1) \sum_{t_2=1}^{\infty} \left(1 - \left(1 - \frac{1}{q^{t_2}}\right)^{m-\lambda}\right) \quad (32)$$

$$< \sum_{t_1=1}^{\infty} t_1 P(T_r = t_1) \sum_{k=1}^{m-\lambda} (-1)^{k-1} \binom{m-\lambda}{k} \frac{1}{q^k - 1} \quad (33)$$

$$< ET_{UB} \left( \sum_{k=1}^{m-\lambda} (-1)^{k-1} \binom{m-\lambda}{k} \frac{1}{q^k - 1} \right) \quad (34)$$

$$\triangleq \rho_{\lambda, UB} \quad (35)$$

Let  $\rho_{UB} = \max\{\rho_{1, UB}, \dots, \rho_{m-1, UB}\}$ . For a sink  $r$ , Let the number of sinks that share at least one parent with  $r$  be  $\Delta$ , then  $\Delta = d - 1 - \binom{n-m}{m}$ . Thus, the middle term in Eq. (20) is bounded by  $\frac{\Delta}{d} \rho_{UB} + \frac{d-1-\Delta}{d} E^2[T_r]$  and

$$\text{var}[T_{\text{avg}}] < \frac{(ET^2)_{UB}}{d} + \frac{\Delta}{d} \rho_{UB} - \left(\frac{\Delta+1}{d}\right) ET_{LB}^2. \quad (36)$$

Depending on the relative values of  $n$  and  $m$ , we have the following three cases.

- $n > 2m$ , then  $\binom{n-m}{m} = \frac{(n-m)!}{m!(n-2m)!}$ , and

$$\frac{\Delta}{d} = 1 - \frac{1}{d} - \frac{\binom{n-m}{m}}{d} \quad (37)$$

$$= 1 - \frac{1}{d} - \frac{(n-m)!(n-m)!}{n!(n-2m)!} \quad (38)$$

$$= 1 - \frac{1}{d} - \frac{(n-m)(n-m-1)\dots(n-2m+1)}{n(n-1)\dots(n-m+1)} \quad (39)$$

$$= 1 - \frac{1}{d} - \left(\frac{n-m}{n}\right) \dots \left(\frac{n-2m+1}{n-m+1}\right) \quad (40)$$

$$< 1 - \frac{1}{d} - \left(\frac{n-2m+1}{n-m+1}\right)^m. \quad (41)$$

Observe from Eqs. (16) and (19) that all of the upper-bound and lower-bound constants are functions of  $m$  and  $q$  only. If  $m$  and  $q$  are fixed and  $n$  increases, in Eq. (41), both  $\frac{\Delta}{d}$  and  $\frac{\Delta+1}{d}$  approaches 0. Therefore,  $\text{var}(T)$  diminishes to 0. Combining this result with the upper-bound  $ET_{UB}$ , we can conclude that, when  $m$  is fixed, even if more intermediate nodes are added, a large proportion of the sink nodes can still be decoded within a small number of coding rounds.

- $n = 2m$ , then  $\binom{n-m}{m} = 1$ ,  $\frac{\Delta}{d} = 1 - \frac{2}{d}$ , and

$$\begin{aligned} \text{var}[T_{\text{avg}}] &< \frac{(ET^2)_{UB}}{d} + \left(1 - \frac{2}{d}\right) \rho_{UB} - \left(1 - \frac{1}{d}\right) ET_{LB}^2 \\ &< \frac{(ET^2)_{UB}}{d} + \rho_{UB} - \left(1 - \frac{1}{d}\right) ET_{LB}^2 \end{aligned} \quad (42)$$

Here  $m$  and  $n$  are comparable in scale, and the bounds depend on the exact values of  $ET_{UB}^2$ ,  $\rho_{UB}$  and  $ET_{UB}$ . We will illustrate through simulation in Section V-A that in this case,  $T_{\text{avg}}$  also converges to 0.

- $n < 2m$ , then  $\binom{n-m}{m} = 0$ ,  $\frac{\Delta}{d} = 1 - \frac{1}{d}$ , and

$$\text{var}[T_{\text{avg}}] < \frac{(ET^2)_{UB}}{d} + \rho_{UB} - ET_{LB}^2, \quad (43)$$

similar to the second case above.

Comparing with the deterministic BNC by Xiao et al. [8], we can see that, for a large combination network, with fixed  $q$  and  $m$ , ARCNC achieves much lower first decoding time. In BNC, the block length is required to be  $p \geq n - m$  at minimum; the decoding delay increases at least linearly with  $n$ , where as in ARCNC, the expected average first decoding time is independent of the value of  $n$ . On the other hand, with RLNC [3], the multicast capacity can be achieved with probability  $(1 - d/q)^n$ . The exponent  $n$  is the number of links with random coefficients; since each intermediate node has the source as a single parent, coding is performed at the source only, and coded data are transmitted on the  $n$  outgoing arcs from the source. When  $q$  and  $m$  are fixed, the success probability of RLNC decreases exponentially in  $n$ . Thus, an exponential number of trials is needed to find a successful RLNC. Equivalently, RLNC can use an increasingly large field size  $q$  to maintain the same decoding probability.

So far we have used  $\binom{n}{m}$  combination networks explicitly to illustrate the operations and the decoding delay gains of ARCNC. It is important to note, however, that this is a very restricted family of networks, in which only the source is required to code, and each sink shares at least 1 parent with other  $\binom{n}{m} - \binom{n-m}{m} - 1$  sinks. In terms of memory, if sink  $r$  cannot decode, all sinks related to  $r$  are required to increase their memory capacity. Recall from Subsection III-C that a non-source node  $v$  is said to be related to a sink  $r$  if  $v$  is an ancestor of  $r$ , or if  $v$  shares a non-source ancestor with  $r$ . As  $n$  becomes larger, the number of nodes related to  $r$  increases, especially if  $m$  increases too. Thus, in combination networks, we do not see considerable gains in terms of memory overheads when compared with BNC, unless  $m$  is small. In more general networks, however, when sinks do not share ancestors with as many other sinks, ARCNC can achieve gains in terms of memory overheads as well, in addition to decoding delay. As an example, we define a *sparsified combination network* next.

## B. Regular sparsified Combination Network

We define a regular sparsified combination network as a modified combination network, with only *consecutive* intermediate nodes connected to unique sink nodes. The framed component in Fig. 4 illustrates its structure. Source  $s$  multicasts  $m$  independent messages through  $m$  intermediate nodes to each sink, with  $n - m + 1$  sinks in total. This topology can be viewed as an abstraction of a content distribution network, where the source distributes data to intermediate servers, and clients are required to connect to  $l$  servers closest in distance to collect enough degrees of freedom to obtain the original data content. This network can be arbitrarily large in scale.



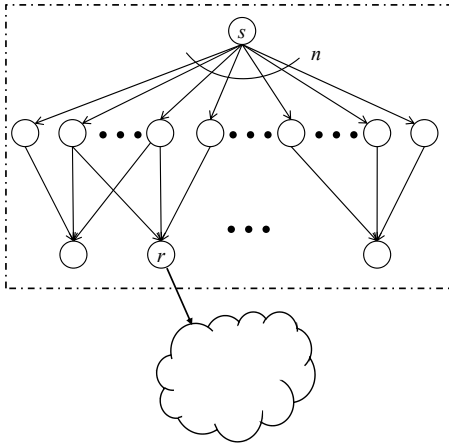


Fig. 4. A regular sparsified combination network (inside the dotted frame) with an extension.

In a regular sparsified combination network, the number of other sinks related to a sink  $r$  is fixed at  $2(m-1)$ , and is even smaller if  $r$ 's parents are on the edge of the intermediate layer. Thus, the average first decoding time of sinks in a regular sparsified combination network behaves similarly to the fixed  $m$  case discussed in the previous subsection, approaching 0 as  $n$  goes to infinity.

On other hand, since now each intermediate node is connected to a fixed number of  $m$  sinks as well, when a sink  $r$  fails to decode and requests an increment in code length, a maximum of  $m + 2(m-1) = 3m - 2$  related nodes are required to increase their memory capacity. To compute  $W_{\text{avg}}$  using Eq. (9), observe that for a sink  $r$ , assuming there are the maximum number of  $2(m-1)$  other sinks related to  $r$ , the cumulative probability distribution of  $L_r$  is as follows

$$\begin{aligned} \Pr\{L_r < t\} &= \Pr\{T_{r-m+1} < t, \dots, T_r < t, \dots, T_{r+m-1} < t\} \\ &= \Pr\{T_{r-m+1} < t\} \Pr\{T_{r-m+2} < t | T_{r-m+1} < t\} \\ &\quad \dots \Pr\{T_{r+m-1} < t | T_{r-m+1} < t, \dots, T_{r+m-2} < t\} \\ &= Q \left(1 - \frac{1}{q^t}\right)^{2m-2} \end{aligned}$$

where  $Q$  is defined in Eq. (10). Thus, using the derivation from Eq. (11) to (16), we have

$$\begin{aligned} E[L_r] &= \sum_{t=1}^{\infty} P(L_r \geq t) \\ &= \sum_{t=1}^{\infty} \left(1 - \prod_{i=1}^m \left(1 - \frac{1}{q^{tr}}\right) \left(1 - \frac{1}{q^t}\right)^{2m-2}\right) \\ &< ET_{UB}(3m-2, q) \end{aligned}$$

Similarly, for an intermediate node  $v$ , we can bound  $E[L_v]$  by  $ET_{UB}(2m, q)$ . Clearly  $W_{\text{avg,ARCNC}}$  computed using Eq. (9) is a function of  $m$  and  $q$  only, independent of  $n$ . In other words, in a regular sparsified combination network, since each sink has a fixed number of parents, and are related to a fixed number of other sinks through its parents, the average amount of memory used across the network is independent of  $n$ .

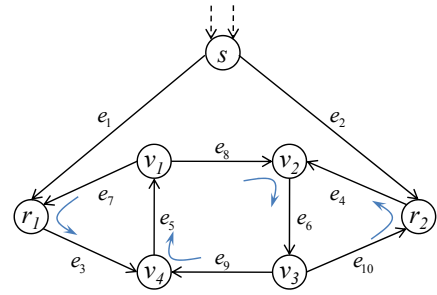


Fig. 5. The shuttle network. Each link has unit capacity.  $s$  is the source;  $r_1$  and  $r_2$  are sinks each with a min-cut of 2. Edges are directed and labeled as  $e_i$ ,  $1 \leq i \leq 10$ . Edges indices are assigned according to Section II-C. An adjacent pair  $(e', e)$  is labeled with a curved pointer if  $e' \geq e$ .

On the other hand, assume a field size of  $q_R$  is used for RLNC code generation. There is a single coding node in the network, with  $n-m+1$  sinks. To guarantee an overall success probability larger than  $1 - \varepsilon$ , we have  $(1 - \frac{n-m+1}{q_R-1})^2 > 1 - \varepsilon$  from [17]. Hence

$$E[W_{\text{avg,RLNC}}] = \lceil \log_2 q_R \rceil > \left\lceil \log_2 \left(1 + \frac{n-m+1}{1 - \sqrt{1-\varepsilon}}\right) \right\rceil,$$

which can be very large if  $n$  is large and  $\varepsilon$  is small.

Comparing the lower-bound on  $E[W_{\text{avg,RLNC}}]$  and the upper-bound on  $E[W_{\text{avg,ARCNC}}]$ , we see that the gain of ARCNC over RLNC in terms of memory use is infinite as  $n$  increases because  $E[W_{\text{avg,ARCNC}}]$  is bounded by a constant value.

An intuitive generalization of this observation is to extend this regular sparsified combination network by attaching another arbitrary network off one of the sinks, as shown in Fig. 4. Regardless of the depth of this extension from the sink  $r$ , as  $n$  increases, memory overheads can be significantly reduced with ARCNC when compared with RLNC, since most of the sinks and intermediate nodes are unrelated to  $r$ , thus not affected by the decodability of sinks within the extension.

### C. Shuttle Network

In this section, we illustrate the use of ARCNC in cyclic networks by applying it to a shuttle network, shown in Fig. 5. We do not provide a formal definition for this network, since its topology is given explicitly by the figure. Source  $s$  multicasts to sinks  $r_1$  and  $r_2$ . Edges  $e_i$ ,  $1 \leq i \leq 10$ , are directed. The edge indices have been assigned according to Section II-C. An adjacent pair  $(e', e)$  is labeled with a curved pointer if  $e' \geq e$ . There are three cycles in the network; the left cycle is formed by  $e_3$ ,  $e_5$ , and  $e_7$ ; the middle cycle is formed by  $e_5$ ,  $e_8$ ,  $e_6$ , and  $e_9$ ; the right cycle is formed by  $e_4$ ,  $e_6$ , and  $e_{10}$ . In this example, we use a field size  $q = 2$ . At node  $v$ , the local encoding kernel matrix is  $K_v(z) = (k_{e',e}(z))_{e' \in In(v), e \in Out(v)} = K_{v,0} + K_{v,1}z + K_{v,2}z^2 + \dots$ ; each local encoding kernel is a polynomial,  $k_{e',e}(z) = k_{e',e,0} + k_{e',e,1}z + k_{e',e,2}z^2 + \dots$ . At  $s$ , assume  $f_{e_1}(z) = \begin{pmatrix} 1 \\ 0 \end{pmatrix}$ , and  $f_{e_2}(z) = \begin{pmatrix} 0 \\ 1 \end{pmatrix}$ , i.e., the data symbols sent out from  $s$  at time  $t$  are  $y_{e_1,t} = x_{1,t}$  and  $y_{e_2,t} = x_{2,t}$ , respectively. The source can also linearly combine source symbols before transmitting on outgoing edges.

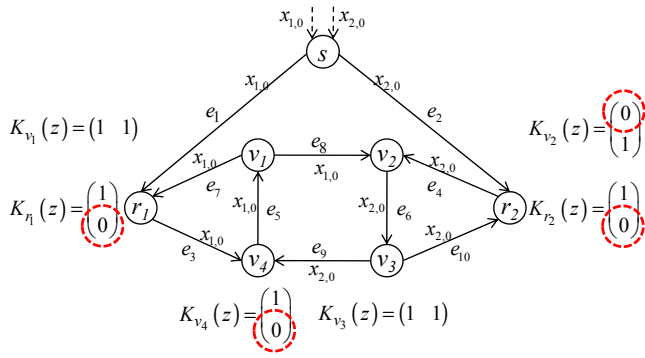


Fig. 6. An example of local encoding kernel matrices at  $t = 0$ . For a node  $v$ ,  $K_v(z) = (k_{e',e}(z))_{e' \in In(v), e \in Out(v)} = K_{v,0} + K_{v,1}z + K_{v,2}z^2 + \dots$ . For any adjacent pair  $(e', e)$  where  $e' \succeq e$ ,  $k_{e',e,0} = 0$ . Each edge  $e$  is labeled with the data symbol  $y_{e,t}$  it carries, e.g.,  $y_{e_1,0} = x_{1,0}$ .

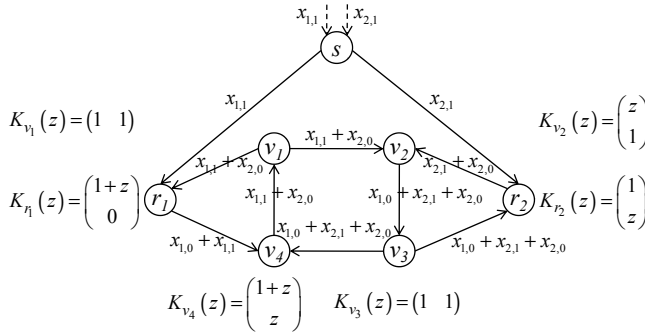


Fig. 7. An example of local encoding kernel matrices at  $t = 1$ .

At  $t = 0$ , we assign 0 to local encoding kernel coefficients  $k_{e',e,0}$  if  $e' \succeq e$ ; and choose  $k_{e',e,0}$  uniformly randomly from  $\mathbb{F}_2$  otherwise. One possible assignment is given in Fig. 6. Here we circle  $k_{e',e,0}$  if  $e' \succeq e$ . Since  $q = 2$ , we set all other local encoding kernel coefficients to 1. The data messages transmitted on each edge at  $t = 0$  are then derived and labeled on the edge. Observe that,  $r_1$  receives  $x_{1,0}$  and  $r_2$  receives  $x_{2,0}$ ; neither is able to decode both source symbols. Hence no acknowledgment is sent in the network.

At  $t = 1$ , we proceed as in the acyclic case, randomly choosing coefficients  $k_{e',e,1}$  from  $\mathbb{F}_2$ . Since no acknowledgment has been sent by  $r_1$  or  $r_2$ , all local encoding kernels increase in length by 1. One possible coding kernel coefficient assignment is given in Fig. 7. Both  $v_1$  and  $v_3$  have one incoming edge only and thus route instead of code, i.e.,  $K_{v_1}(z) = K_{v_3}(z) = (1 \ 1)$ . The other local encoding kernel matrices in this example are as follows

$$\begin{aligned}
K_{r_1,1}(z) &= \begin{pmatrix} k_{e_1,e_3,0} \\ k_{e_7,e_3,0} \end{pmatrix} + \begin{pmatrix} k_{e_1,e_3,1} \\ k_{e_7,e_3,1} \end{pmatrix} z = \begin{pmatrix} 1 \\ 0 \end{pmatrix} + \begin{pmatrix} 1 \\ 0 \end{pmatrix} z, \\
K_{r_2,1}(z) &= \begin{pmatrix} k_{e_2,e_4,0} \\ k_{e_{10},e_4,0} \end{pmatrix} + \begin{pmatrix} k_{e_2,e_4,1} \\ k_{e_{10},e_4,1} \end{pmatrix} z = \begin{pmatrix} 1 \\ 0 \end{pmatrix} + \begin{pmatrix} 0 \\ 1 \end{pmatrix} z, \\
K_{v_4,1}(z) &= \begin{pmatrix} k_{e_3,e_5,0} \\ k_{e_9,e_5,0} \end{pmatrix} + \begin{pmatrix} k_{e_3,e_5,1} \\ k_{e_9,e_5,1} \end{pmatrix} z = \begin{pmatrix} 1 \\ 0 \end{pmatrix} + \begin{pmatrix} 1 \\ 1 \end{pmatrix} z, \\
K_{v_2,1}(z) &= \begin{pmatrix} k_{e_4,e_6,0} \\ k_{e_8,e_6,0} \end{pmatrix} + \begin{pmatrix} k_{e_4,e_6,1} \\ k_{e_8,e_6,1} \end{pmatrix} z = \begin{pmatrix} 0 \\ 1 \end{pmatrix} + \begin{pmatrix} 1 \\ 0 \end{pmatrix} z.
\end{aligned}$$

Data symbols generated according to Eq. (5) for this particular code are also labeled on the edges. For example, on edge  $e_5 = (v_4, v_1)$ , the data symbol transmitted at  $t = 1$  is

$$\begin{aligned}
y_{e_5,1} &= y_{e_3,0}k_{e_3,e_5,1} + y_{e_3,1}k_{e_3,e_5,0} \\
&\quad + y_{e_9,0}k_{e_9,e_5,1} + y_{e_9,1}k_{e_9,e_5,0} \\
&= x_{1,0} \cdot 1 + (x_{1,0} + x_{1,1}) \cdot 1 + x_{2,0} \cdot 1 + y_{e_9,1} \cdot 0 \\
&= x_{1,1} + x_{2,0}
\end{aligned} \tag{44}$$

Observe that there are no logical contradictions in any of the three cycles. For example, in the middle cycle, on  $e_5$ , regardless of the value of  $y_{e_9,1}$ , the incoming data symbol at  $t = 1$ ,  $y_{e_5,1}$ , can be evaluated as in Eq. (44). In other words, in evaluating the global encoding kernel coding coefficients according to Eqs. (3) and (4), even though  $f_{e_9,1}$  is unknown,  $f_{e_5,1}$  can still be computed since  $k_{e_9,e_5,0} = 0$ .

Also from Fig. 7, observe that both sinks can decode two source symbols at  $t = 1$ :  $r_1$  can decode  $x_{1,1}$  and  $x_{2,0}$ , while  $r_2$  can decode  $x_{2,1}$  and  $x_{1,0}$ . Equivalently, we can compute the global encoding kernel matrices and check the decodability conditions given in Section II-B. We omit the details here, but interested readers can verify using Eq. (3) that the global encoding matrices are  $F_{r_1}(z) = \begin{pmatrix} 1 & 1 \\ 0 & z \end{pmatrix}$ ,  $F_{r_2}(z) = \begin{pmatrix} 0 & z \\ 1 & 1+z \end{pmatrix}$ , and the decodability conditions are indeed satisfied. Acknowledgments are sent back by both sinks to their parents, code lengths stop to increase, and ARCNC terminates. The first decoding time for both sinks is therefore  $T_{r_1} = T_{r_2} = 1$ .

As we have discussed in Section II-C, the deterministic edge indexing scheme proposed is an universal but heuristic way of assigning local encoding kernel coefficients at  $t = 0$ . In this shuttle network example, observe from Fig. 6 that in the middle cycle composed of edges  $e_8$ ,  $e_6$ ,  $e_9$  and  $e_5$ , this scheme introduces two zero coefficients, i.e.,  $k_{e_8,e_6,0} = 0$ , and  $k_{e_9,e_5,0} = 0$ . A better code would be to allow one of these two coefficients to be non-zero. For example, if  $k_{e_8,e_6,0} = 1$ ,  $K_{v_2}(z) = \begin{pmatrix} 1 \\ 1 \end{pmatrix}$  at  $t = 0$ . It can be shown in this case that the data symbol transmitted on  $e_{10}$  to  $r_2$  is  $y_{e_{10},0} = x_{1,0} + x_{2,0}$ , enabling  $r_2$  to decode both source symbols at time  $t = 0$ .

## V. SIMULATIONS

We have shown analytically that ARCNC converges in finite steps with probability 1, and that it can achieve gains in decoding time or memory in combination networks. In what follows, we want to verify these results through simulations, and to study numerically whether similar behaviors can be observed in random networks. We implemented the proposed encoder and decoder in MATLAB. In all instances, it can be observed that decoding success was achieved in a finite amount of time. All results plotted in this section are averaged over 1000 runs.

### A. Combination Network

Recall from Section IV-A that an upper bound  $ET_{UB}$  and a lower bound  $ET_{LB}$  for the average expected first decoding time  $E[T_{\text{avg}}]$  can be computed for a  $\binom{n}{m}$  combination network. Both are functions of  $m$  and  $q$ , independent of  $n$ . In evaluating  $\text{var}[T_{\text{avg}}]$ , three cases were considered,  $n > 2m$ ,  $n = 2m$ , and

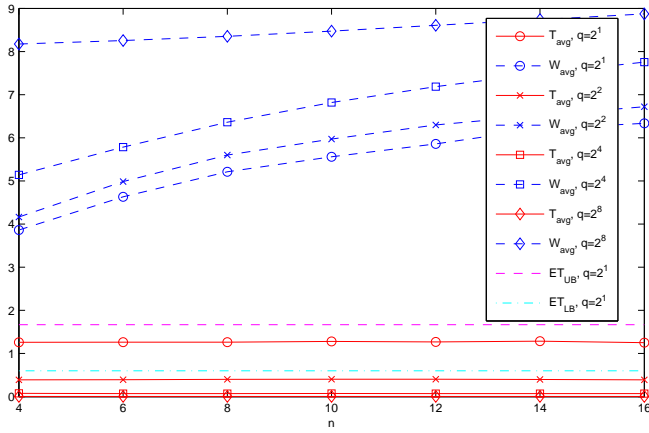


Fig. 8. Average first decoding time and average memory use.  $m = 2$ ,  $n$  increases, field size  $q$  also increases. Also plotted are the computed upper and lower bounds on  $T_{\text{avg}}$  for  $q = 2$ .

$n < 2m$ . When  $n > 2m$ , the number of sinks unrelated to a given sink  $r$  is significant. If it takes  $r$  multiple time steps to achieve decodability, not all other sinks and intermediate nodes have to continue increasing their encoding kernel length to accommodate  $r$ . Thus, ARCNC can offer gains in terms of decoding delay and memory use. We show simulation results below for the case when  $m$  is fixed at the value of 2, while  $n$  increases. By comparison, if  $n \leq 2m$ , there is a maximum of one sink related to a given sink  $r$ . We show simulation results below for the case of  $n = 2m$ .

1)  $n > 2m$ , fixed  $m$ ,  $m = 2$ : Fig. 8 plots the average first decoding time  $T_{\text{avg}}$ , corresponding upper and lower bounds  $ET_{UB}$ ,  $ET_{LB}$ , and average memory use  $W_{\text{avg}}$ , as defined in Section III-C. Here  $m$  is fixed to the value of 2,  $n$  increases from 4 to 16, and the field size is  $q = 2$ . As discussed in Section IV-A,  $ET_{UB}$  and  $ET_{LB}$  are independent of  $n$ . As  $n$  increases, observe that  $T_{\text{avg}}$  stays approximately constant at about 1.3, while  $W_{\text{avg}}$  increases sublinearly. When  $n = 16$ ,  $W_{\text{avg}}$  is approximately 6.3. On the other hand, recall from [17] that a lower bound on the success probability of RLNC is  $(1 - d/(q-1))^{|J|+1}$ , where  $|J|$  is the number of encoding nodes. In a combination network with  $n = 16$  and  $m = 2$ ,  $|J| = 1$  since only the source node codes. For a target decoding probability of 0.99, we have  $(1 - \binom{16}{2}/(q-1))^2 \geq 0.99$ , thus  $q > 2.4 \times 10^4$ , and  $\lceil \log_2 q \rceil \geq 15$ . Since each encoding kernel contains at least one term,  $W_{\text{avg}}$  is lower bounded by  $\lceil \log_2 q \rceil$ . Hence, using ARCNC here reduces memory use by half when compared with RLNC.

Fig. 8 also plots  $T_{\text{avg}}$  and  $W_{\text{avg}}$  when field size  $q$  increases from  $2^1$  to  $2^8$ . As field size becomes larger,  $T_{\text{avg}}$  approaches 0. When  $q = 2^8$ , the value of  $T_{\text{avg}}$  is close to 0.004. As discussed in Section IV-A, when  $q$  becomes sufficiently large, ARCNC terminates at  $t = 0$ , and generates the same code as RLNC. Also observe from this figure that as  $n$  increases from 4 to 16,  $W_{\text{avg}}$  increases as well, but at different rates for different field sizes. Again,  $W_{\text{avg}}$  is lower bounded by  $\lceil \log_2 q \rceil$ . When  $q = 2^8$ ,  $W_{\text{avg}}$  follows an approximately linear trend, with an increment of less than 1 between  $n = 4$  and  $n = 16$ . One explanation for this observation is that for  $m = 2$ , a

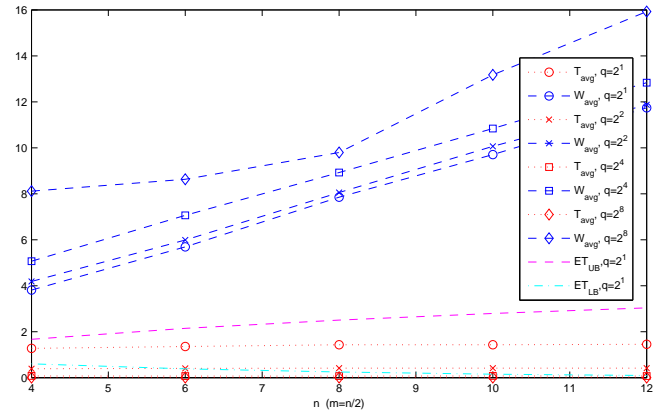


Fig. 9. Average first decoding time and average memory use.  $n = 2m$ ,  $n$  increases, field size  $q$  also increases. Also plotted are the computed upper and lower bounds on  $T_{\text{avg}}$  for  $q = 2$ .

field size of  $q = 2^8$  is already sufficient for making ARCNC approximately the same as RLNC.

2)  $n = 2m$ : Fig. 9 plots  $T_{\text{avg}}$ ,  $W_{\text{avg}}$ , and corresponding bounds on  $T_{\text{avg}}$  when  $n = 2m$ ,  $q = 2$ . Since  $m$  increases with  $n$ ,  $ET_{UB}$  and  $ET_{LB}$  change with the value of  $n$  as well. Observe that  $T_{\text{avg}}$  increases from approximately 1.27 to approximately 1.45 as  $n$  increases from 4 to 12. In other words, even though more sinks are present, with each sink connected to more intermediate nodes, the majority of sinks are still able to achieve decodability within very few coding steps. However, since now  $n = 2m$ , any given sink  $r$  is related to all but one other sink; even a single sink requiring additional coding steps would force almost all sinks to use more memory to store longer encoding kernels. Compared with Fig. 9,  $W_{\text{avg}}$  appears linear in  $n$  in this case.

Fig. 9 also plots  $T_{\text{avg}}$  and  $W_{\text{avg}}$  when  $q$  increases. Similar to the  $m = 2$  case shown in Fig. 9,  $T_{\text{avg}}$  approaches 0 as  $q$  becomes larger.  $W_{\text{avg}}$  appears linear in  $n$  for  $q \leq 2^6$ , and piecewise linear for  $q = 2^8$ . This is because  $W_{\text{avg}}$  is lower bounded by  $\lceil \log_2 q \rceil$ . When  $n$  becomes sufficiently large, this lower bound is surpassed, since  $q = 2^8$  no longer suffices in making all nodes decode at time 0, thus making ARCNC a good approximation of RLNC.

## B. Shuttle Network

When there are cycles in the network, as discussed in Section II-C, we numerically index edges, and assign local encoding kernels at  $t = 0$  according to the indices such that no logical contradictions exist in data transmitted around each cycle. Fig. 10 plots  $T_{\text{avg}}$  and  $W_{\text{avg}}$  for the shuttle network, with the index assignment given in Fig. 5. As discussed in the example shown in Figs. 6 and 7, with this edge index index, both  $r_1$  and  $r_2$  require at least 2 time steps to achieve decodability. This conclusion is verified by the plot shown in Figure 10. As field size  $q$  increases,  $T_{\text{avg}}$  converges to 1, while  $W_{\text{avg}}$  converges to  $2 \log_2 q$ . When  $q = 2^1$ ,  $T_{\text{avg}}$  is 5.1.

## C. Acyclic and Cyclic Random Geometric Networks

To see the performance of ARCNC in random networks, we use random geometric graphs [18] as the network model,

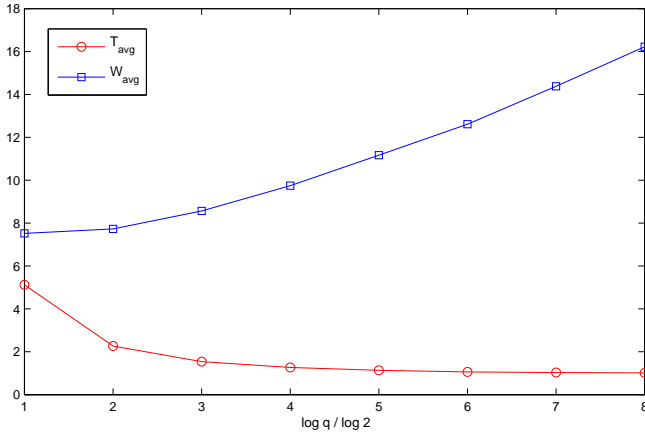


Fig. 10. Average decoding delay and average code length for the shuttle network as a function of field size.

with added acyclic or cyclic constraints. In random geometric graphs, nodes are put into a geometrically confined area  $[0, 1]^2$ , with coordinates chosen uniformly randomly. Nodes which are within a given distance are connected. Call this distance the connection radius. In our simulations, we set the connection radius to 0.4. The resulting graph is inherently bidirectional.

For acyclic random networks, we number all nodes, with source as node 1, and sinks as nodes with the largest numbers. A node is allowed to transmit to only nodes with numbers larger than its own. An intermediate node on a path from the source to a sink can be a sink itself. To ensure the max-flow to each receiver is non-zero, one can choose the connection radius to make the graph connected with high probability; we fix this value to 0.4, and throw away instances where at least one receiver is not connected to the source. Once an acyclic random geometric network is generated, we use the smallest min-cut over all sinks as the source symbol rate, which is the number of source symbols generated at each time instant.

Figs. 11 and 12 plot the average first decoding time  $T_{avg}$  and average memory use  $W_{avg}$  in acyclic random geometric networks. Fig. 11 shows the case where there are 25 nodes within the network, with more counted as sinks, while Fig. 12 shows the case where the number of sinks is fixed to 3, but more nodes are added to the network. In both cases,  $T_{avg}$  is less than 1, indicating that decodability is achieved in 2 steps with high probability. In Fig. 11, the dependence of  $W_{avg}$  on the number of sinks is not very strong, since there are few sinks, and each node is connected to only a small portion of all nodes. In Fig. 12,  $W_{avg}$  grows as the number of nodes increases, since on average, each node is connected to more neighboring nodes, thus its memory use is more likely to be affected by other sinks.

To see the performance of ARCNC in cyclic random networks, note that random geometric graphs are inherently bidirectional. We apply the following modifications to make the network cyclic. First, we number all nodes, with source as node 1, and sinks as the nodes with the largest numbers. Second, we replace each bidirectional edge with 2 directed edges. Next, a directed edge from a lower numbered to a higher numbered node is removed from the graph with probability

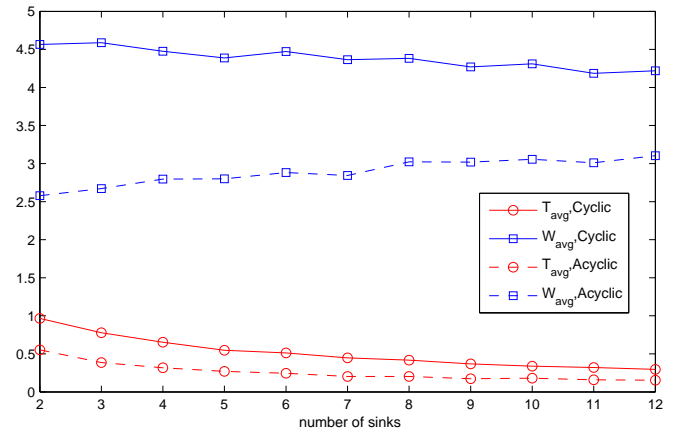


Fig. 11. Average first decoding time and average memory use in acyclic and cyclic random geometric graphs with 25 nodes, as a function of the number of receivers. Field size is  $q = 2^2$ .

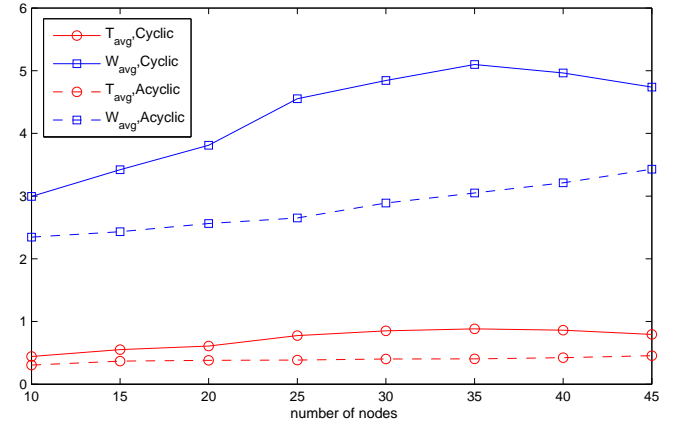


Fig. 12. Average first decoding time and average memory use in a cyclic random geometric graph with 3 receivers, as a function of the total number of nodes in the network. Field size is  $q = 2^2$ .

0.2, and a directed edge from a higher numbered to a lower numbered node is removed from the graph with probability 0.8. Such edge removals ensure that not all neighboring node pairs form cycles, and cycles can exist with positive probabilities. We do not consider other edge removal probabilities in our simulations. The effect of random graph structure on the performance of ARCNC is a non-trivial problem and will not be analyzed in this paper.

Figs. 11 and 12 also plot the average first decoding time and average memory use in cyclic random geometric networks. Again, in both cases, the average first decoding time  $T_{avg}$  is less than 1, indicating that decodability is achieved in 2 steps with high probability.  $W_{avg}$  stays approximately constant when more nodes becomes sinks. On the other hand, when the number of sinks is fixed to 3, while more nodes are added to the network,  $W_{avg}$  first increases, then decreases in value. This is because as more nodes are added, since the connection radius stays constant at 0.4, each node is connected to more neighboring nodes. Sharing parents with more nodes first increase the memory use of a given node. However, as more nodes are added and more cycles form, edges are utilized

more efficiently, thus bringing down both  $T_{\text{avg}}$  and  $W_{\text{avg}}$ . Note that when compared with the acyclic case, cyclic networks with the same number of nodes or same number of sinks require longer decoding time as well as more memory. This is expected, since with cycles, sinks are related to more nodes in general.

## VI. CONCLUSION

We propose an adaptive random convolutional network code (ARCNC), operating in a small field, locally and automatically adapting to the network topology by incrementally growing the constraint length of the convolution process. Through analysis and simulations, we show that ARCNC performs no worse than random algebraic linear network codes in terms of decodability, while bringing significant gains in terms of decoding delay and memory use in some networks. There are three main advantages of ARCNC compared with scalar network codes and conventional convolutional network codes. Firstly, it operates in a small finite field, reducing the computation overheads of encoding and decoding operations. Secondly, it adapts to unknown network topologies, both acyclic and cyclic. Lastly, it allows codes of different constraint lengths to co-exist within a network, thus bringing practical gains in terms of smaller decoding delays and reduced memory use. The amount of gains achievable through ARCNC is dependent on the number of sinks connected to each other through mutual ancestors. In practical large-scale networks, the number of edges connected to an intermediate node or a sink is always bounded. Thus ARCNC could be beneficial in most general cases.

One possible extension of this adaptive algorithm is to consider its use with other types of connections such as multiple multicast, or multiple unicast. Another possible direction of future research is to understand the impact of memory used during coding on the rates of innovative data flow through paths along the network. ARCNC presents a feasible solution to the multicast problem, offering gains in terms of delay and memory, but it is not obvious whether a constraint can be added to memory, while jointly optimizing rates achievable at sinks through this adaptive scheme.

## REFERENCES

- [1] R. Ahlswede, N. Cai, S. Li, and R. Yeung, "Network information flow," *IEEE Trans. on Info. Theory*, vol. 46, no. 4, pp. 1204–1216, 2000.
- [2] R. Li, S.Y.R. Yeung and N. Cai, "Linear network coding," *IEEE Trans. on Info. Theory*, vol. 49, no. 2, pp. 371–381, 2003.
- [3] T. Ho, M. Médard, R. Koetter, D. Karger, M. Effros, J. Shi, and B. Leong, "A random linear network coding approach to multicast," *IEEE Trans. on Info. Theory*, vol. 52, no. 10, pp. 4413–4430, 2006.
- [4] M. Médard, M. Effros, D. Karger, and T. Ho, "On coding for non-multicast networks," in *Proc. of the 41st Allerton Conference*, vol. 41, no. 1, 2003, pp. 21–29.
- [5] S. Jaggi, P. Sanders, P. Chou, M. Effros, S. Egner, K. Jain, and L. Tolhuizen, "Polynomial time algorithms for multicast network code construction," *IEEE Trans. on Info. Theory*, vol. 51, no. 6, pp. 1973–1982, 2005.
- [6] S. Li and R. Yeung, "On convolutional network coding," in *Proc. of IEEE Int. Sym. on Info. Theory*, 2006, pp. 1743–1747.

- [7] E. Erez and M. Feder, "Convolutional network codes," in *Proc. of IEEE Int. Sym. on Info. Theory (ISIT)*, 2005, p. 146.
- [8] M. Xiao, M. Médard, and T. Aulin, "A binary coding approach for combination networks and general erasure networks," in *Proc. of IEEE Int. Sym. on Info. Theory (ISIT)*, 2008, pp. 786–790.
- [9] W. Guo, N. Cai, X. Shi, and M. Medard, "Localized dimension growth in random network coding: A convolutional approach," in *Proc. of IEEE Int. Sym. on Info. Theory (ISIT)*, 2011, pp. 1156–1160.
- [10] T. Ho, S. Jaggi, S. Vyetrenko, and L. Xia, "Universal and robust distributed network codes," in *2011 IEEE Proceedings of INFOCOM*, 2010, pp. 766–774.
- [11] C. Ngai and R. Yeung, "Network coding gain of combination networks," in *Proc. of IEEE Info. Theory Workshop*, 2004, pp. 283–287.
- [12] N. Cai and W. Guo, "The conditions to determine convolutional network coding on matrix representation," in *Proc. NetCod*, 2009, pp. 24–29.
- [13] J. Massey and M. Sain, "Inverses of linear sequential circuits," *IEEE Trans. on Comp.*, vol. 100, no. 4, pp. 330–337, 2006.
- [14] W. G. Guo, N. Cai, and Q. T. Sun, "Time-Variant Decoding of Convolutional Network Codes," *IEEE Communications Letters*, vol. 16, no. 10, pp. 1656–1659, 2012.
- [15] R. Yeung, S. Li, N. Cai, and Z. Zhang, "Network Coding Theory: Single Sources," *Foundations and Trends® in Communications and Information Theory*, vol. 2, no. 4, pp. 241–329, 2005.
- [16] R. Koetter and M. Médard, "An algebraic approach to network coding," *IEEE/ACM Trans. on Networking*, vol. 11, no. 5, pp. 782–795, 2003.
- [17] H. Balli, X. Yan, and Z. Zhang, "On randomized linear network codes and their error correction capabilities," *IEEE Trans. on Info. Theory*, vol. 55, no. 7, pp. 3148–3160, 2009.
- [18] M. Newman, "Random graphs as models of networks," *Handbook of Graphs and Networks*, pp. 35–68, 2003.